water

MDPI

Article

Structure and Physicochemical Properties of Water Treated under Carbon Dioxide with Low-Temperature Low-Pressure Glow Plasma of Low Frequency

Aleksandra Ciesielska [1], Wojciech Ciesielski [2,*], Karen Khachatryan [3], Henryk Koloczek [4], Damian Kulawik [2], Zdzisław Oszczeda [5], Jacek Soroka [6] and Piotr Tomasik [5]

1 Faculty of Chemistry, University of Gdansk, Wita Stwosza St. 63, 80-308 Gdansk, Poland; olaciesielska5@gmail.com
2 Institute of Chemistry, Jan Długosz University, Armii Krajowej Ave. 13–15, 42-201 Częstochowa, Poland; d.kulawik@ujd.edu.pl
3 Faculty of Food Technology, University of Agriculture in Krakow, Balicka Str. 122, 30-149 Krakow, Poland; rrchacza@cyf-kr.edu.pl
4 Institute of Chemistry and Inorganic Technology, Krakow University of Technology, Warszawska Str. 24, 31-155 Krakow, Poland; koloczek@indy.chemia.pk.edu.pl
5 Nantes Nanotechnological Systems, Dolnych Młynów Str. 24, 59-700 Bolesławiec, Poland; z.oszczeda@nantes.com (Z.O.); rrtomasi@cyf-kr.edu.pl (P.T.)
6 Scientific Society of Szczecin, Wojska Polskiego Street 96, 71-481 Szczecin, Poland; Jacek.Soroka@zut.edu.pl
* Correspondence: w.ciesielski@interia.pl

Received: 17 June 2020; Accepted: 3 July 2020; Published: 6 July 2020

Abstract: Treatment of water saturated with CO_2 with low-temperature, low-pressure glow plasma of low-frequency (GP) produced a series of liquids. Their temperature and intensity of thermal effects non-linearly depended on the treatment time. However, the Raman spectra patterns of the treated water pointed to a specific structure of the water treated for 30 min. The spectra of control, non-treated water saturated with CO_2, and such water treated for 15, 60, 90, and 120 min showed that their macrostructure was built mainly by a single donor, and single hydrogen bonded arrangements accompanied, to a certain extent, with free water molecules. The macrostructure of the water treated for 30 min consisted chiefly of tetrahedral and deformed tetrahedral structural units. That water contained long-living free radicals of discussed structure, stabilized in such macrostructure.

Keywords: carbon dioxide clathrates; solvent niches; carbon dioxide-free radical; carbonic acid; cold plasma interaction

1. Introduction

Our recent papers have presented macrostructure and properties of water treated with low-temperature and low-pressure glow plasma of low-frequency (GP) in the air [1] as well as under pure nitrogen [2], ammonia [3], and methane [4]. The GP-treated water, generally called nanowater, exhibits several interesting functional properties. They depend on the mode of preparation. Nanowater stimulates various fermentative microorganisms, biopesticides and drastically influences the production of essential oils by herbs, control breeding plants, and animals. Such applications have been recently reviewed in our recent paper [5]. Physicochemical studies [1–5] have revealed that in every case, the treatment of water with GP results in declusterization of the water macrostructure, and molecules of gases dissolved in the treated water are excited. In such states, they are closed inside aqueous clathrates. In every case, the extent to which water is declusterized and the structure of resulting clathrates, as well as their excited guest molecules, depend on the treatment time and

intensity of relaxation processes occurring between the preparation of samples. In such a manner, a series of nanowaters suitable for many applications has become available.

In this paper, the structure and properties of water treated with GP under carbon dioxide were presented.

The CO_2 gas is quite soluble in water. It reaches 0.0770 mol/kg (0.335 w%) at 0 °C and decreases proportionally against temperature to 0.0198 mol/kg water at 50 °C under normal pressure [6]. More than 99% CO_2 exists as the dissolved gas and less than 1% as carbonic acid, H_2CO_3, partly dissociated into the H^+, HCO_3^-, and CO_3^{2-} ions [7]. According to Knoche [7], since carbon dioxide can hydrate and twice dissociate in water, the reaction Scheme (1) may be written as

$$\begin{array}{cccc} & k_1 & & k_2 \\ CO_2 + H_2O < ==> & H_2CO_3 & <==> & HCO_3^- + H^+ <==> CO_3^{2-} + 2H^+ \\ & k_{-1} & & k_{-2} \end{array} \quad (1)$$

The equilibrium is determined by the three equilibrium constants (Equations (2)–(4))

$$K_h = \frac{[H_2CO_3]}{[CO_2][H_2O]} \quad (2)$$

$$K_{al} = \frac{\left[H_2CO_3^-\right]\left[H^+\right]\cdot f_{2+}}{[H_2CO_3]} \quad (3)$$

$$K_{a2} = \frac{\left[CO_3^{2-}\right][H^+]^2\cdot f_{2-}\cdot f_+}{\left[H_2CO_3^-\right]\cdot f_-} \quad (4)$$

and by the total concentration of CO_2 (c_{tot}) present in solution given in Equation (5)

$$ctot = [CO_2] + [H_2CO_3] + [HCO_3^-] + [CO_3^{2-}] \quad (5)$$

where f_i is the activity coefficient. Activities of the uncharged species CO_2 and H_2CO_3 are commonly taken to be equal to their concentrations, and the activity of water is unity. Although the full evidence for this scheme is not yet available, it is clearly more general than the "classical" reaction scheme [8].

There are several papers that have described the hydration of CO_2 [9–14] and dehydration of H_2CO_3 [15,16]. Interestingly, CO_2 forms clathrates with water. Usually, low temperature and elevated pressure are required for their formation [17]. Clathrate hydrates are cage-like structures of water molecules that house guest gas species. Less readily, such clathrates are formed in the presence of mineral compounds, for instance, $MgSO_4$ [18]. Such properties may be utilized for the storage of CO_2 as well as the evolution of methane from its aqueous clathrates [17,19]. Such direction of the application of aqueous CO_2 clathrates additionally underlined the importance of our studies presented in this paper.

2. Materials and Methods

2.1. Treating Water with GP

Distilled water (200 mL) in a glass flask was placed in the chamber of the reactor [20]. Through the deionized water, a stream of pure (100%) CO_2 (AIR-PRODUCTS, Warsaw, Poland) was bubbled and exposed to interaction with plasma for 5, 15, 30, 60, and 90 min. The plasma of 38 °C was generated at 5×10^{-3} mbar, 600 V, 50 mA, and 10 kHz frequency. The produced water was stored at ambient temperature in 100 mL closed Teflon^{TM} containers.

2.2. Physicochemical Properties of GP-Treated Water

2.2.1. pH

pH was taken using a laboratory multifunction meter Cx-505 (Elmetron, Zabrze, Poland) equipped with a combined calomel-glass electrode. The resolution of the instrument was 0.01 pH. Measurements were performed at 25 °C. The estimations were run in triplicates.

2.2.2. Conductivity

Measurements were performed in triplicates at 25 °C with an ELMETRON CPC-505 instrument (Elmetron, Zabrze, Poland) equipped in an ELMETRON EC-60 sensor.

2.2.3. Differential Scanning Calorimetry (DSC)

Differential scanning calorimeter DSC 204F1 Phoenix (Netzsch, Selb, Germany) was used. Multipoint calibration (Hg, In, Sn, Bi, Zn, CsCl) was involved. Twelve milligrams of samples were analyzed by heating them from 20 to 140 °C at the rate of 5 °C/min. Characteristic temperatures and enthalpy of transitions (T_{onset}, T_{mid}, T_{end}, and ΔH) were determined with Proteus Analysis (Netzsch, Selb, Germany) software.

2.2.4. Refractive Index

For measurements, a lab refractometer RL from PZO Warsaw, Poland, was used. Its resolution was 0.0002. The measurements were run in triplicates.

2.2.5. Fourier Transformation Infrared—Attenuated Total Reflectance (FTIR-ATR) Spectra

The FTIR-ATR spectra of the film were recorded in the range of 700–4000 cm^{-1} at a resolution of 4 cm^{-1} using a Mattson 3000 FT-IR (Madison, WI, USA) spectrophotometer. That instrument was equipped with a 30SPEC 30° reflectance adapter fitted with the MIRacle ATR accessory from PIKE Technologies Inc., Madison, WI, USA.

2.2.6. Electron Spin Resonance (ESR) Spectra

The spectra were recorded at room temperature, employing an instrument constructed at Wroclaw Technical University. The range of the X-band (ν = 9.5 GHz, λ = 3.158 cm) was employed at the 20–25 dB attenuation and 2048 s swiping time. An ESR controller software designed for taking the ESR spectra was applied and recorded in the form of the first derivative.

2.2.7. Ultraviolet/Visible (UV-VIS) Spectra

The spectra were recorded with a Thermo Scientific Evolution Spectrometer 220 (Thermo Fisher Scientific, Waltham, MA, USA) spectrophotometer in the wavelength range of 190–1100 nm in a quartz gas-tight cell of 10 mm path length.

2.2.8. Raman Spectra

The spectra were taken with a Perkin-Elmer MPF44A Fluorescence Spectrophotometer (Waltham, MA, USA) equipped with a xenon lamp and 4 mL quartz cell. The sample was excited at 330 ± 1 nm at 20 °C, and both slits were set on 2 nm. The spectra were recorded in wavelength scale and then recalculated to wavenumber scale shifted to value excitation energy.

3. Results and Discussion

Treatment of water saturated with CO_2 with GP produced a series of liquids. Their onset temperature and intensity of thermal effects depended on the treatment time, as shown by Differential

Scanning Calorimetry (DSC) (Table 1). These parameters varied non-linearly against the treatment time. Likely, the number of nucleation centers decreased against temperature increase.

Table 1. Thermodynamic data for GP-treated deionized water saturated with CO_2.

Sample	Onset Temperature (°C)	Peak Maximum (°C)	Peak Abruption [b] (PA) (1/°C)	Enthalpy ΔH (J/g)	Entropy ΔS (J/g K)	Maximum of Heat Flow (MHF) (W/g)
W [a]	98.60	99.20	1.67	−1645.3	2.69765	4.729
WCO_20 [c]	98.40	99.90	0.67	−1649.2	2.71564	5.144
WCO_25	100.50	101.20	1.43	−1666.5	2.72456	5.000
WCO_215	102.60	103.30	1.43	−1621.8	2.63452	4.263
WCO_230	104.10	104.90	1.25	−1603.4	2.44545	3.240
WCO_260	101.90	102.20	3.33	−1632.5	2.61242	5.084
WCO_290	102.30	102.80	2.00	−1658.7	2.67977	4.787
WCO_2120	101.40	102.00	1.67	−1674.2	2.71863	5.558

[a] Control, deionized water prior to its saturation with CO_2 and GP treatment. [b] Reciprocal of **Δ**T peak maximum and onset temperatures. [c] WCO_20 = water saturated with CO_2 treated for 0 min.

Saturation of water with CO_2 resulted in a decrease in the onset temperature solely by 0.2 °C and increase in peak maximum by 0.7 °C. The treatment of water with GP for initial 5 min increased temperature of the onset temperature and the peak maximum by further 2.1 and 1.3 °C, respectively. GP treatment prolonged to 30 min increased relevant temperatures by 5.7 and 5.0 °C, respectively. Further GP treatment increased the values of those parameters practically linearly with respect to one another. However, the values of those parameters elevated nonlinearly against the treatment time in the orders:

Onset temp: $WCO_20 < W < WCO_25 < WCO_2120 < WCO_260 < WCO_290 < WCO_215 < WCO_230$
Peak temp: $W < WCO_20 < WCO_25 < WCO_2120 < WCO_260 < WCO_290 < WCO_215 < WCO_230$

Water treated for 15 and 30 min demonstrated the highest onset and peak temperatures. These changes were associated with changes in enthalpy, entropy, and the value of the accompanying thermal effect measured for particular samples. They changed in the following orders (see Table 1 for notation):

ΔH: $WCO_2120 < WCO_25 < WCO_290 < WCO_20 < W < WCO_260 < WCO_215 < WCO_230$
ΔS: $WCO_230 < WCO_260 < WCO_215 < WCO_290 < W < WCO_20 < WCO_2120 < WCO_25$
MHF: $WCO_230 < WCO_215 < W < WCO_290 < WCO_25 < WCO_260 < WCO_20 < WCO_2120$
PA: $WCO_20 < WCO_230 < WCO_215 < WCO_25 < W = WCO_2120 < WCO_290 < WCO_260$

These orders were linear neither with respect to one another nor against the treatment time. Again, samples of water treated for 30 and 15 min closed the H order and opened the S and MHF orders.

Initially, the homogenous macrostructure of water reflected by a high value of PA was perturbed by the saturation of water with CO_2. Several niches were formed to store the CO_2 molecules.

The introduced disorder was reflected by the lowest PA value. The GP treatment evoked a continuous transformation from one macrostructure into another, and the condition of the thermodynamic stability was not the ruling factor. It is known [21–26] that the CO_2 molecule is linear in the free state but bend in the first electronic excited state in order to decrease the total energy of the molecule. This phenomenon could contribute to these irregularities as the given way of involvement of CO_2 in constructing macrostructure could selectively favor excitation of the molecule. The GP treatment led to the homogenous distribution of niches holding the CO_2 molecules as indicated by increasing PA values. Finally, very compact, polymeric macrostructure was formed as indicated by a gradually increasing energy of evaporation.

Saturation of deionized water with CO_2 resulted in a slight decrease in pH of the solution, which was accompanied by a considerable increase in its conductivity. The original pH of non-treated water saturated with CO_2 was practically insensitive to the GP treatment (Table 2). After an initial

increase in conductivity, the treatment with GP provided practically linear subtle—linear against the treatment time—increase in that parameter (Table 2).

Table 2. The pH and conductivity of deionized water saturated with CO_2 depending on glow-plasma (GP) treatment.

Treatment Time (min)	pH	Conductivity (mS/cm)
Water	7.00 ± 0.02	0.092 ± 0.003
0	6.85 ± 0.02	1.005 ± 0.007
5	6.85 ± 0.04	1.008 ± 0.008
15	6.84 ± 0.03	1.073 ± 0.005
30	6.78 ± 0.02	1.098 ± 0.012
60	6.79 ± 0.03	1.118 ± 0.002
90	6.84 ± 0.04	1.141 ± 0.003
120	6.91 ± 0.05	1.154 ± 0.004

These results suggested that prolonged GP treatment provided a gradual surrounding of the CO_2 molecules with water, which inhibited their hydration and dissociation. An increase in conductivity might suggest that some ions, for instance, either hydronium ions or the hydroxyl groups, were not engaged in specific interactions, decreasing their mobility. Besides, some residual ions present in the deionized water could be involved.

In the region of 200–350 nm, the UV-VIS spectra (Figure 1) of the deionized water, non-saturated with CO_2, and prior to the treatment with GP revealed solely a low shoulder (A = 0.05 a.u at 200 nm) of a peak located below 200 nm. After the GP treatment, regardless of the treatment time (0, 5, 15, 30, 60, 90, 120 min), the samples saturated with CO_2 developed absorption band at 200 nm. The intensity of that band, originating from the $n \rightarrow \pi^*$ transitions in the solvated CO_2 molecule, was independent of the treatment time reaching A = 1.35 ± 0.05 a.u. at 200 nm. Thus, the concentration of CO_2 in particular samples was independent of the GP treatment time. Besides, the measured refractive index (n^{20}_D = 1.3330) was independent of the GP treatment time, indicating no changes in electron concentration (stability of chemical concentration, the stability of density) of the liquid phase.

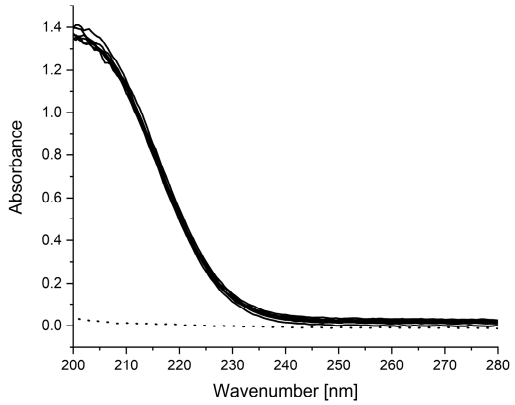

Figure 1. UV-VIS spectra of the deionized water, non-saturated with CO_2, and prior to the treatment with GP (pointed line) and after the GP treatment (solid lines). GP, glow plasma of low frequency.

The FTIR-ATR reflectance spectrum of deionized water free of CO_2 and saturated with CO_2 is presented in Figure 2. The absorbance of the bands at around 1600 ($\nu_{s\,C=O}$), 1300 ($\nu_{s\,C-O}$), and 1100 (δ_{OH}) cm^{-1} in the spectra of particular GP-treated samples showed that the carbonic acid dissociation depended on the GP treatment time in a non-linear manner.

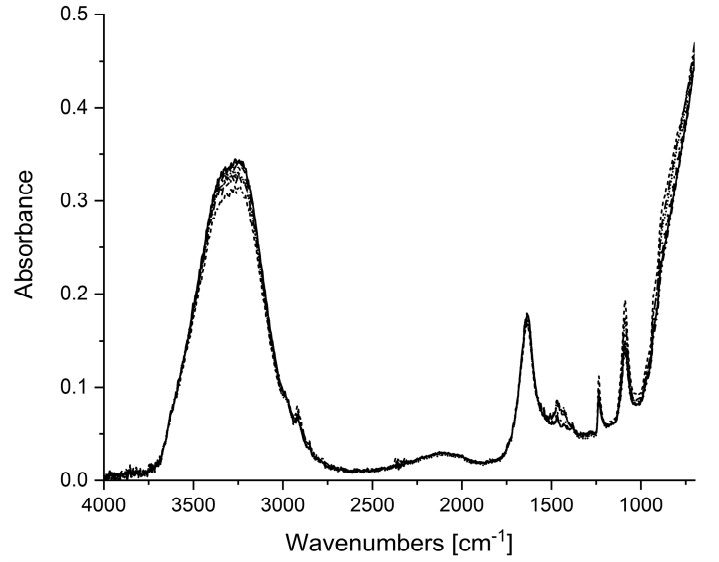

(**a**)

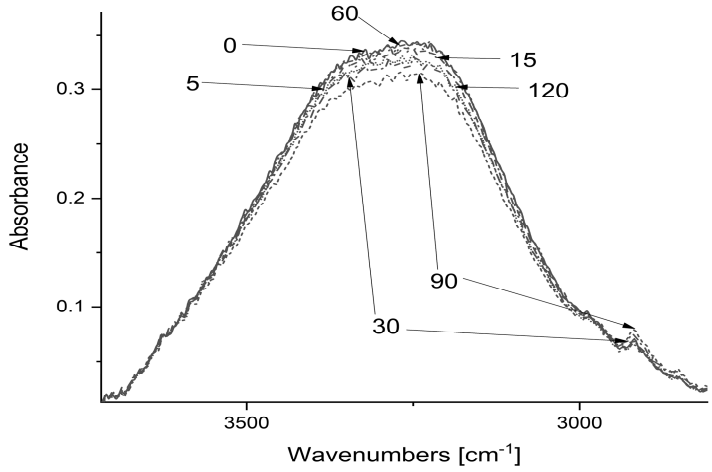

(**b**)

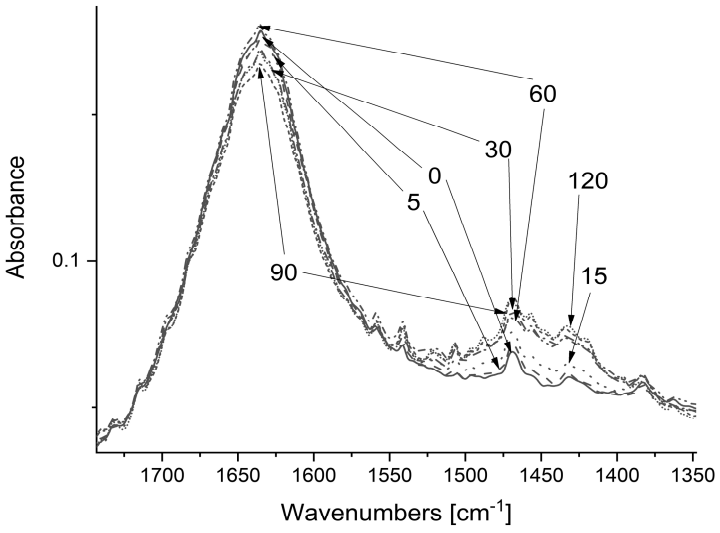

(**c**)

Figure 2. *Cont.*

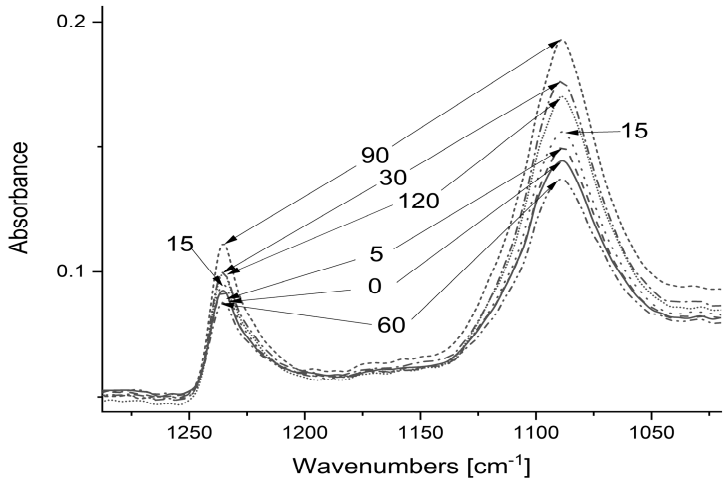

(**d**)

Figure 2. The FTIR reflectance spectra of deionized water and such water saturated with CO_2 and treated with GP for 0–120 min: (**a**) the fundamental spectrum, (**b**–**d**) particular sectors of the spectra separately enlarged. Consult Table 3 for assigning band intensities to the given sample.

Table 3. The absorbance of the OH stretching (bands A and B), ν_{OH}, bending (band C), δ_{OH}, modes in the FTIR spectra of water saturated with CO_2 taken in the region of 1500–4000 cm^{-1}.

Water Plasming Time (min)	A(3480)	B(3260)	C(1635)	A/B	A/C	B/C
0	0.1140	0.3393	0.1781	0.3360	0.6401	1.9051
5	0.0961	0.3318	0.1746	0.2896	0.5504	1.9003
15	0.0961	0.3307	0.1781	0.2906	0.5396	1.8568
30	0.1000	0.3193	0.1720	0.3132	0.5814	1.8564
60	0.1080	0.3318	0.1810	0.3255	0.5967	1.8331
90	0.0832	0.3113	0.1675	0.2673	0.4967	1.8585
120	0.0941	0.3264	0.1719	0.2883	0.5474	1.8988

The strong peak in the region of 3000–3550 cm^{-1} represented ν_{OH} band composed, in fact, of several overlapped bands belonging to symmetric and asymmetric OH vibrations of water and carbonic acid. However, about 1% concentration of carbonic acid was not essential for attempts of separation of that band into components belonging to asymmetric and symmetric stretching vibrations belonging to water. For that purpose, following Chaplin [27], the Gaussian separation of that band into two bands was performed, representing asymmetric (band A) and symmetric (band B) components (Figure 3).

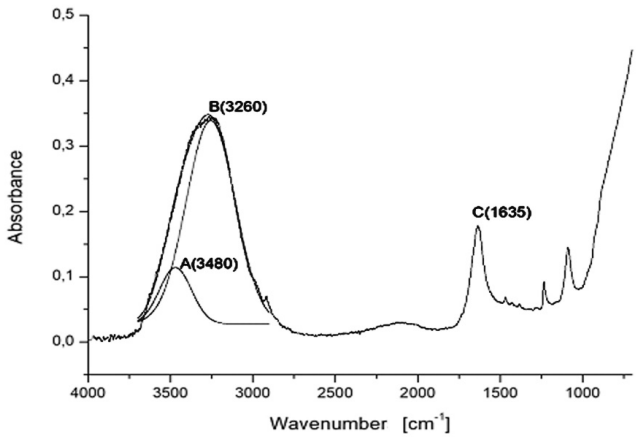

Figure 3. The result of the Gaussian distribution of the ν_{OH} band in the FTIR spectrum of water.

The A- and B-bands represented water molecules vibrating asymmetrically and symmetrically, respectively. The C-band corresponded to the bending modes of the OH–group (δ_{OH}). In the spectra of water treated with GP in the air, after the 5 min treatment, the number of asymmetrically vibrating molecules was the highest. It added weak hydrophobic properties to that water [1]. In contrast to that, the GP treatment of water saturated with CO_2, regardless of the treatment time, always reduced the number of asymmetrically vibrating water molecules. Again, the extent of that reduction non-linearly depended on the treatment time (Table 3). The treatment time had no distinct effect on the pattern of the spectrum, but it influenced the intensity ration of the corresponding bands (A/B, A/C, and B/C). It spoke in favor of the influence of the treatment time on the water macrostructure and the equilibria (2)–(4). Additionally, the effect of the GP treatment upon the structure of CO_2 should be taken into account. The peak around 2900 cm^{-1} represented an artifact resulting from the imprecise subtraction of the background in our single-beam spectrophotometer. A low band at around 2343 cm^{-1} reflected vibrations in dissolved CO_2. The intensity of that band was identical for all samples under study.

In our recent papers [1–3], the formation of clathrated singlet oxygen [1], triplet nitrogen [2], and ammonia [3] in water was postulated as the result of the treatment of water in contact with the air, under nitrogen, and under ammonia, respectively. Such a conclusion was drawn based on the pattern of the Raman spectra. The relevant spectra always contained two essential intensive bands in the region 300–450 nm (the wavelengths represented the Raman scattering on excitation at 330 nm).

The Raman spectrum (Figure 4) of original water (1st control) demonstrated a strong peak centered at 3260 cm^{-1} with a shoulder on its long wavelength 3480 cm^{-1}. It was fully adequate with the data presented in Figure 3. The main peak could be assigned [28] to single donor single hydrogen-bonded water and free water, whereas the more energetic shoulder corresponded to deformed tetrahedrally arranged structures. The spectrum of the 2nd control water being the original tap water saturated with CO_2 was significantly less intensive. This effect could partly result from a lower number of water molecules compared to the number of water molecules in 1st control in a given volume of the investigated sample. However, the pattern of that spectrum spoke for a substantial reconstruction of the macrostructure in the sample. The low maximum of broadband was located in the region, corresponding to the spectrum of 1st control to the shoulder, representing tetrahedrally arranged structures. In this spectrum, the band representing symmetrically vibrating single donor single hydrogen-bonded water and free water was represented by a low, flat shoulder. It could also be observed as a shoulder in the spectrum of control water prior to its saturation with CO_2.

Only the shape of the spectrum of the water saturated with CO_2 treated for 30 min did not exhibit the low energetic shoulder. The other spectra of the water saturated with CO_2 treated for 5–120 min resembled the spectrum of 2nd control. However, the intensity of those spectra varied non-linearly against the treatment time. This irregularity fitted the regularities observed in UV and FTIR spectra.

The ESR spectra of the samples revealed a very specific character of the sample treated for 15 and particularly for 30 min. Only these samples developed a signal in the ESR spectrum (Figure 5). The spectrum pointed to a free radical with unpaired spin localized either on the carbon or oxygen atoms.

For an extremely short lifetime, any free radical developed from the single CO_2 molecule could not be observed with the ESR technique. That instability resulted from free rotation around the σ–σ bond. On such rotation by 180°, antibonding orbital turned that orbital into bonding, which would be equivalent to ceasing unpaired electron, i.e., ceasing free radical. However, trapping short-living radicals by another CO_2 molecule would lead to a stable structure, as presented in Figure 5.

Alternative consideration took into account a possibility of the formation of niches, hosting two CO_2 molecules on the GP treatment for 15 and 30 min. Under such circumstances, these two guest molecules could be excited, developing diradical with unpaired spins localized on the oxygen atoms. Such diradical could be stabilized by reaction with one water molecule, providing a unit with its hydrophilic head and hydrophobic tail with two O-diradicals and one likely singlet carbene. That unit could be stabilized by its incorporation into a wall of the niche. Prolonged GP treatment ruined these

structures, separated CO_2 molecules, and in consequence, observed radicals ceased, but it resulted in the development of a more uniform macrostructure (Figure 6).

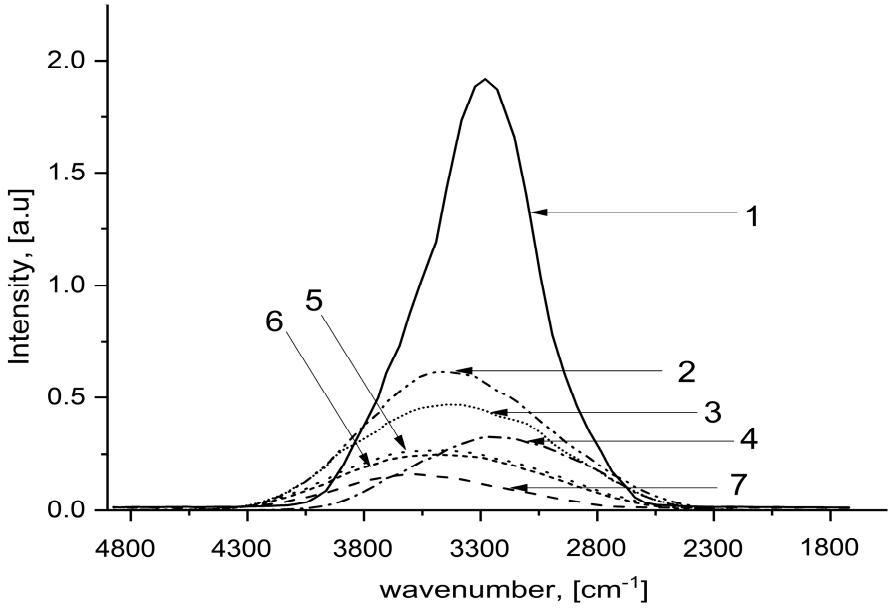

Figure 4. The Raman spectrum (excitation 330 nm) of the water treated with GP for 0 to 120 min. Notation: 1—pure water (primary control); 2—water saturated with CO_2, non-treated (secondary control); 3–7—water treated for 15, 30 60, 90, and 120 min, respectively.

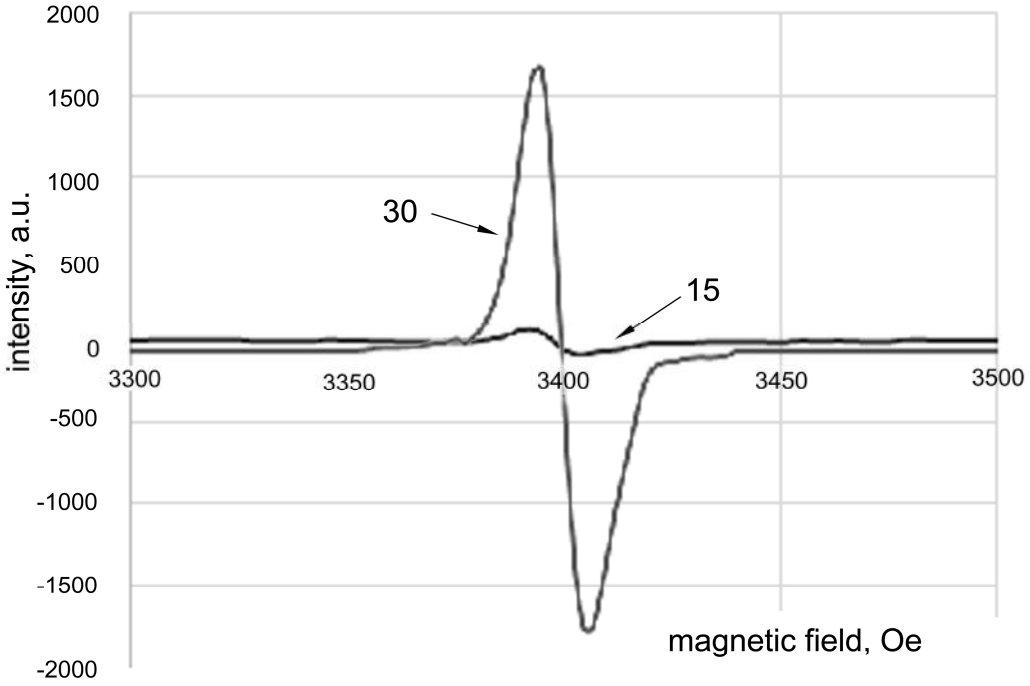

Figure 5. The ESR spectrum of deionized water saturated with CO_2 and then treated with GP for 15 and 30 min.

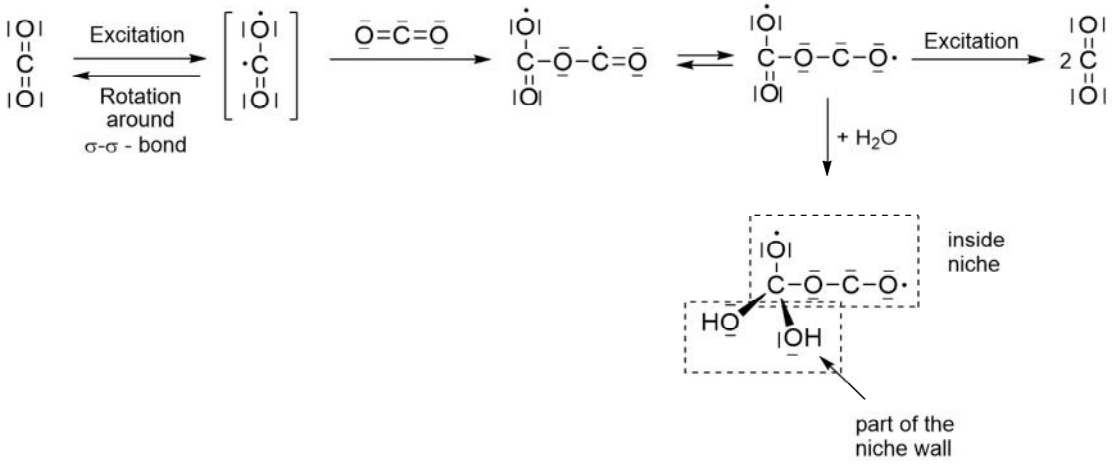

Figure 6. Possible formation and structure of observed free radical.

4. Conclusions

Initially, the homogenous macrostructure of water was perturbed by the saturated water with CO_2. Several niches (clusters) in the macrostructure were formed to store the CO_2 molecules. Transformations of those macrostructures took place on prolonged GP treatment. They involved the varying role of the tetrahedral, deformed tetrahedral, symmetrically vibrating single donor single hydrogen-bonded water, and free water in particular developed macrostructures. Some niches could host two CO_2 molecules. Under such circumstances, the excitation could produce triplet CO_2, efficiently trapped by a non-excited CO_2 molecule. The oxygen diradical formed in such a manner could be stabilized, interacting with the surface of the cluster. Thus, non-treated water saturated with CO_2 and such water treated with GP for 15 and 30 min formed a specific macrostructure with incorporated free radicals. It consisted chiefly of tetrahedral and deformed tetrahedral structural units, including O-free radicals formed of carbon dioxide stabilized in the macrostructure by bonding to the walls of niches. Prolonged GP treatment ruined these structures. Particular CO_2 molecules hosted in isolated niches and dimeric radical decomposed into two singlet CO_2 molecules. As a consequence, observed radicals ceased, but simultaneously, the macrostructure turned more homogenous.

Author Contributions: A.C. run pH, conductivity measurements, W.C. run ESR spectra, K.K. run UV-VIS and Infrared Spectra, H.K. run Raman spectra, D.K. run thermogravimetry measurements, Z.O. equipped a research team in nanowater, P.T. invented the project, coordinated study and designed the text of this report, J.S. run substantial remarks and discussion of the subject. All authors jointly participated in interpretation of all data and in writing report. All authors have read and agreed to the published version of the manuscript.

Funding: This research did not receive any specific grant from funding agencies in the public, commercial, or not-for-profit sectors.

Conflicts of Interest: The authors declare no conflict of interest.

References

1. Białopiotrowicz, T.; Ciesielski, W.; Domański, J.; Doskocz, M.; Fiedorowicz, M.; Grąż, K.; Khachatryan, K.; Kołoczek, H.; Kozak, A.; Oszczęda, Z.; et al. Structure and physicochemical properties of water treated with low-temperature low-frequency plasma. *Curr. Phys. Chem.* **2016**, *6*, 312–320. [CrossRef]
2. Chwastowski, J.; Ciesielska, K.; Ciesielski, W.; Khachatryan, K.; Koloczek, H.; Kulawik, D.; Oszczeda, Z.; Tomasik, P.; Witczak, M. Structure and physicochemical properties of water treated under nitrogen with low-temperature glow plasma of low frequency. *Water* **2020**, *12*, 1314. [CrossRef]
3. Ciesielska, K.; Ciesielski, W.; Khachatryan, K.; Koloczek, H.; Kulawik, D.; Oszczeda, Z.; Tomasik, P. Structure and physicochemical properties of water treated under ammonia with low pressure low-temperature glow plasma of low-frequency. *Glob. Chem. J.* **2020**. submitted.

4. Ciesielska, A.; Ciesielski, W.; Khachatryan, K.; Kołoczek, H.; Kulawik, D.; Oszczęda, Z.; Soroka, J.A.; Tomasik, P. Structure and physicochemical properties of water treated under methane with low-temperature glow plasma of low frequency. *Water* **2020**, *12*, 1638. [CrossRef]
5. Tomasik, P.; Oszczęda, Z. Application of water treated with low-pressure, low-temperature glow plasma (nanowater) in food and cosmetic technology (in Polish) Prom. *Zdr. Ekol.* **2019**, *4*, 21–28.
6. Hamad, H.S.; Davies, R. The ionization constant of carbonic acid in water and the solubility of carbon dioxide in water and aqueous salt solutions from 0° to 50 °C. *J. Am. Chem. Soc.* **1943**, *65*, 2030–2037.
7. Knoche, W. Chemical reactions of CO_2 in water. In *Biophysics and Physiology of Carbon Dioxide*; Bauer, C., Gros, G., Barteis, H., Eds.; Springer: Berlin/Heidelberg, Germany, 1980; pp. 3–11.
8. Gibbons, B.H.; Edsall, J.T. Rate of hydration of carbon dioxide and dehydration of carbonic acid at 25 °C. *J. Biol. Chem.* **1963**, *238*, 3502–3507.
9. Kern, D.M. The hydration of carbon dioxide. *J. Chem. Educ.* **1960**, *37*, 14–23. [CrossRef]
10. Ho, C.; Sturtevant, J.M. The kinetics of the hydratation of carbon dioxide at 25 °C. *J. Biol. Chem.* **1963**, *238*, 3499–3501. [PubMed]
11. Magid, E.; Turnbeck, B.O. The rates of the spontaneous hydration of CO_2 and the reciprocal reaction in neutral aqueous solutions between 0° and 38°. *Biochim. Biophys. Acta* **1968**, *165*, 515–524. [CrossRef]
12. Patel, R.C.; Boe, R.J.; Atkinson, G. The CO_2-water system, Part I. *J. Sol. Chem.* **1973**, *2*, 367–372.
13. Nguyen, M.T.; Matus, M.H.; Jackson, V.E.; Vu, T.N.; Rustad, J.R.; Dixon, D.A. Mechanism of the hydration of carbon dioxide: Direct participation of H_2O versus microsolvation. *J. Phys. Chem. A* **2008**, *112*, 10386–10398. [CrossRef] [PubMed]
14. England, A.H.; Duffin, A.M.; Schwartz, C.P.; Uejio, J.S.; Prendergast, D.; Saykally, R.J. On the hydration and hydrolysis of carbon dioxide. *Chem. Phys. Lett.* **2011**, *514*, 187–195. [CrossRef]
15. Rossi-Bernardi, L.; Berger, R.L. The rapid measurements of pH by the glass electrode. The kinetics ofdehydration of carbonic acid at 25 °C and 37 °C. *J. Biol. Chem.* **1968**, *243*, 1297–1302.
16. Yarris, L. New Insight on Carbonic Acidm in Water, Berkeley Lab. Available online: https://newscenter.lbl.gov/2014/10/22/new-insights-on-carbonic-acid-in-water/ (accessed on 10 June 2020).
17. Jadhawar, P.; Mohammadi, A.H.; Yang, J.; Tohidi, B. Subsurface carbon dioxide storage throughout clathrate hydrate formation. In *Advances in the Geological Storage of Carbon Dioxide*; Nato Sciences Ser. IV, Earth and Environmental Sciences; Lombardi, S., Altunina, L.K., Beaubien, S.E., Eds.; Springer: Dordrecht, The Netherlands, 2006; Volume 65, pp. 111–126.
18. Safi, E.; Thompson, S.P.; Evans, A.; Day, S.J.; Murray, C.A.; Parker, J.E.; Baker, A.R.; Oliveira, J.M.; van Loon, J.T. Properties of CO_2 clathrate hydrates formed in the presence of $MgSO_4$ solutions with implications for icy moons. *Astron. Astrophys.* **2017**, *600*, A88. [CrossRef]
19. Jadhawar, P.; Park, Y.; Kim, D.-Y.; Lee, J.-W.; Huh, D.-G.; Park, K.-P.; Lee, J.; Lee, H. Sequestering carbon dioxide into complex structures of naturally occurring gas hydrates. *Proc. Natl. Acad. Sci. USA* **2006**, *103*, 12690–12694.
20. Oszczeda, Z.; Elkin, I.; Strek, W. Equipment for treatment of water with plasma. Polish Patent PL 216025 B1, 28 February 2014.
21. McDiarmid, R.; Doering, J.P. Electronic excited states of CO_2-An electron impact investigation. *J. Chem. Phys.* **1984**, *80*, 648–656. [CrossRef]
22. Crabtree, R.H. *The Organometallic Chemistry of the Transition Metals*, 6th ed.; J. Wiley: Hoboken, NJ, USA, 2014; p. 145.
23. Spielfiedel, A.; Feautrier, N.; Cossart-Magos, C.; Chambaud, G.; Rosmus, P.; Werner, H.J.; Botschwina, P. Bent valence excited states of CO_2. *J. Chem. Phys.* **1992**, *97*, 8382–8388. [CrossRef]
24. Hitchcock, A.P.; Brian, C.E.; van der Wiel, C.E. Ionic fragmentation of inner shell excited states of CO_2 and N_2O. *Chem. Phys. Lett.* **1979**, *66*, 213–217. [CrossRef]
25. Knowles, P.J.; Rosmus, P.; Werner, H.-J. On the assignment of the electronically excited states in linear CO_2. *Chem. Phys. Lett.* **1988**, *146*, 230–235. [CrossRef]
26. Luccini, M.; Murari, M.; Lucarelli, G.D.; Frasetto, F.; Poletto, L.; Schnappinger, T.; de Vivie-Riedle, R.; Nisoli, M. Observation of ultrafast dynamics in CO_2 highly excited states. In Proceedings of the European Conference on Lasers and Electro-Optics 2019, Munich, Germany, 23–27 June 2019.

27. Chaplin, M. Water Structure and Science. Available online: www1.lsbu.ac.uk/water/water_vibrational_spectrum.html (accessed on 15 September 2016).
28. Hu, Q.; Zhao, H.; Ouyang, S. Understanding water structure from Raman spectra of isotopic substitution H_2O/D_2O up to 573 K. *Phys. Chem. Chem. Phys.* **2017**, *19*, 21540–21547. [CrossRef] [PubMed]